Deep-Learning-Based Imaging through Glass-Air Disordered Fiber with Transverse Anderson Localization

Jian Zhao,[1,*] Yangyang Sun,[1] Zheyuan Zhu,[1] Donghui Zheng,[1,2] Jose Enrique Antonio-Lopez,[1] Rodrigo Amezcua Correa,[1] Shuo Pang[1] and Axel Schülzgen[1]

[1]*CREOL, College of Optics and Photonics, University of Central Florida, Orlando, FL 32816, USA*
[2]*School of Electronic and Optical Engineering, Nanjing University of Science and Technology, Nanjing, Jiangsu 210094, China*
**Corresponding author: JianZHAO@knights.ucf.edu*

Abstract: We demonstrate for the first time that deep neural networks (DNNs) can be trained to recover images transported through a 90 cm-long silica-air disordered optical fiber at variable working distances without any distal optics.
OCIS codes: (060.2280) Fiber design and fabrication; (060.2310) Fiber Optics; (060.4005) Microstructured fibers

1. Introduction

The guiding of light through disordered optical fibers based on transverse Anderson localization (TAL) has been investigated in detail in recent years [1-5]. An optical beam can propagate along the disordered optical fiber while maintaining a finite beam cross-section due to the TAL effect caused by strong random scattering in the transverse plane. Recent studies on polymer Anderson localized fiber have proved that the image transport quality obtained in the disordered optical fiber can be comparable to or better than some of the best commercial multicore imaging fibers [2], and the transversally localized states of the disordered fiber show single mode properties [3]. Compared to the polymer disordered fiber, the glass-air Anderson localized optical fibers (GALOFs) are expected to have even better performance in image transport due to lower loss of the glass materials and much smaller beam point spread function [4]. In a recent study, bending-independent image transport through 90 cm-long fiber has been demonstrated [5], which shows great potential for practical applications, such as endoscopes for biological and medical imaging. However, the structural parameters of current GALOFs are still less than perfect, which limits the quality of transported images. In addition, previous experiments are limited to the transportation of images that are located directly at the GALOF's input facet unless distal optical elements are added. For objects away from the fiber input facet only a blurred image is observed at the proximal facet.

In this work, we demonstrate experimentally that meter-scale GALOFs can transport high-quality images of objects located at various working distances from the fiber input facet. This has been achieved without additional optical components by training of deep neural networks (DNNs). We show the recovery of objects when raw intensity image transported through a 90 cm-long GALOF are provided.

2. DNN training, experiment and results

A DNN attempts to generate a computational architecture that maps all input in a test set to their corresponding outputs based on a given training set (examples of matched input and output data). It has been proven that DNNs can be trained to recover object from diffracted intensity images [6]. In our experiment, images of objects located at different working distances are transported through a 90 cm long GALOF and subsequently recorded by a CCD camera. Object reconstruction process can be described as:

$$X = HY_{measure} \quad , \tag{1}$$

where $Y_{measure}$ is the measured image matrix, X is the reconstructed image matrix. The pair, (X, $Y_{measure}$), corresponds to the test set, and H is an inverse operator that gives an estimation of the original object from the measurement. In past years, obtaining the inverse operator by solving optimization problem has been studied in detail [7,8]. However, it requires accurate modeling and prior knowledge of the object. In contrast, DNNs can learn H from a provided training set and no prior knowledge of the object is required. The method applied here is an extension of a recent DNN study [9] which uses a convolutional residual neural network.

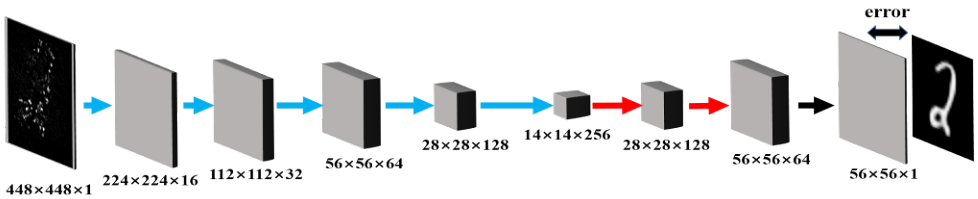

Fig. 1. Schematic of our DNN architecture.

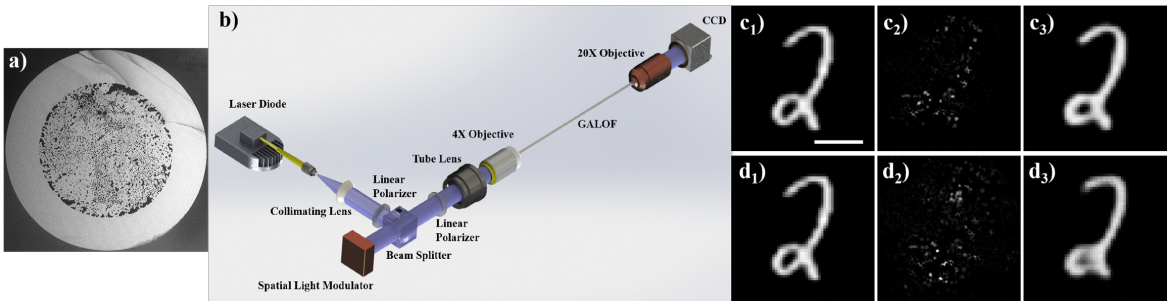

Fig. 2. a) SEM cross-section image of GALOF. The outer diameter is 414 μm and the diameter of the disordered core is 278 μm. The air-hole-fraction in the core is 28.5%. The air-hole feature sizes range from 0.8 μm to over 10 μm with a maximum in the size distribution around 1.6 μm. b) Experimental setup. c_1) and d_1) are objects from the MNIST database of handwritten digits. Image c_1) is projected directly into the GALOF input facet while image d_1) is projected into an imaging plane 2 mm away from the GALOF facet. c_2) and d_2) are the images of c_1) and d_1) after transport through 90 cm-long GALOF, and c3) and d3) are the reconstructed images after DNN training. The scale bar in c_1) is 45 μm.

The architecture of our DNN is shown in Fig.1. The input layer is a 448×448×1 pixel image cropped from the measured image. Then it is successively connected by five residual blocks of convolution+down-sampling (Fig. 1 blue arrows) followed by two residual blocks of deconvolution+up-sampling (Fig. 1 red arrows) and a single final standard residual block (Fig. 1 black arrows). At the very last layers of our DNN, the output represents an estimation of the object. The connection weights are trained by backpropagation on the mean absolute error between the network output images and the nominal appearance of the training images (Fig. 1 double-sided arrow) described as: $|X_{train} - G|/(wh)$, where w and h are the width and height of the output image, X_{train} is the output matrix of the last layer and G is the ground truth value matrix. We adopted an Adam optimizer in tensor flow with batch size of 5, while the learning rate is set to 0.0001. The neural network was trained for 15 epochs with shuffling at each epoch.

The GALOF was fabricated at CREOL using fused-silica rods and tubes and the stack-and-draw method. A SEM image of the GALOF cross-section is shown in Fig. 2(a). The experimental arrangement is shown in Fig. 2(b). The 405 nm laser light delivered by a single mode fiber is collimated by a lens (50mm focal length). Then the light goes through the first polarizer oriented 45° with respect to the extraordinary axis of the spatial light modulator (SLM). The SLM (1920x1152 XY Spatial Light Modulator, Meadowlark Optics) is modulated by 8-bit grayscale input images (MNIST Digits). After reflection from the SLM, the beam goes through a second polarizer with the same polarization orientation as the first one. Then the imaging area of the SLM is projected onto the GALOF input facet by the combination of a tube lens and a 4x objective. At the output end of the GALOF the fiber facet is projected onto CCD by a 20x objective. 1500 images from the MNIST dataset are fed into the system to generate corresponding raw intensity images. These 1500 image pairs are used to train our DNN. The training time is 5 minutes on GPU (GTX 1070 Ti). Another different 500 raw intensity images are collected as the test set. We repeat our experiments and image reconstruction for different working distances. Results for working distances of 0 mm and 2 mm are shown in Fig 2 c) and d), respectively. Fig. 2 c_1)-c_3) and d_1)-d_3) show the original objects, raw intensity images and the corresponding reconstructed images. Comparing c_1) and c_3) as well as d_1) and d_3) it is apparent that our trained DNNs are able to recover the true images remarkably well for both working distances.

3. Conclusion

In conclusion, we demonstrate the first disordered optical fiber based imaging system where a trained DNN is utilized to reconstruct objects located at different working distances using raw intensity images transported through 90 cm of disordered fibers as input data. This approach could be applied to develop novel fiber based imaging systems which can provide artifact-free images from various working distances without any distal optics.

4. References

[1] T. Schwartz, G. Bartal, S. Fishman, and M. Segev, "Transport and Anderson localization in disordered two-dimensional photonic lattices," Nature **446**, 52-55 (2007).
[2] S. Karbasi, R. J. Frazier, K. W. Koch, T. Hawkins, J. Ballato, and A. Mafi, "Image transport through a disordered optical fibre mediated by transverse Anderson localization," Nat. Commun. **5**, 3362 doi:10.1038/ncomms4362 (2014).
[3] G. Ruocco, B. Abaie, W. Schirmacher, A. Mafi, and M. Leonetti, "Disorder-induced single-mode transmission," Nat. Commun. **8**, 14571 doi:10.1038/ncomms14571 (2017).
[4] J. Zhao, J. E. Antonio-Lopez, R. A. Correa, A. Mafi, M. Windeck, and A. Schülzgen, "Image Transport Through Silica-Air Random Core Optical Fiber," in "CLEO: Science and Innovations," (Optical Society of America, 2017), paper JTu5A.91.
[5] J. Zhao, J. E. Antonio-Lopez, R. A. Correa, D. Zheng, and A. Schülzgen, "Image Transport Through Meter-Long Silica-Air Disordered Optical Fiber," 5th Workshop on Specialty Optical Fibers, paper: 10 (2017), to be published in Proceedings SPIE.
[6] A. Sinha, J. Lee, S. Li, and G. Barbastathis, "Lensless computational imaging through deep learning," Optica **4**,1117-1125 (2017).
[7] Y. Sun, X. Yuan, and S. Pang, "High-speed compressive range imaging based on active illumination," Opt. Express **24**, 22836-22846 (2016)
[8] Y. Sun, X. Yuan, and S. Pang, "Compressive high-speed stereo imaging," Opt. Express **25**, 18182-18190 (2017).
[9] R. Horisaki, R. Takagi, and J. Tanida, "Learning-based imaging through scattering media," Opt. Express **24**, 13738-13743 (2016).